RSC Advances

ROYAL SOCIETY OF CHEMISTRY

www.rsc.org/advances

RSCPublishing

ARTICLE

Kinetic modeling of self-aggregation in solutions with coexisting spherical and cylindrical micelles at arbitrary initial conditions

Cite this: DOI: 10.1039/x0xx00000x

Received 00th June 2014,
Accepted 00th xxxxxx 2014

DOI: 10.1039/x0xx00000x

www.rsc.org/

A. K. Shchekin,[a] I. A. Babintsev,[a] L.Ts. Adzhemyan,[a] N. A. Volkov[a]

We have numerically studied the nonlinear dynamics of aggregation of surfactant monomers in a micellar solution. The study has been done on the basis of a discrete form of the Becker-Döring kinetic equations for aggregate concentrations. The attachment/detachment coefficients for these equations were determined from the extended Smoluchowski diffusion model. Three typical situations at arbitrary large initial deviations from the final aggregative equilibrium with coexisting premicellar aggregates, spherical and cylindrical micelles have been considered. The first situation corresponds to micellization in the solution where initially only surfactant monomers were present. Other two situations refer to nonlinear relaxation in the cases of substantial initial excess and deficit of surfactant monomers in solution over their equilibrium concentration in the presence of spherical and cylindrical aggregates. The interplay between non-equilibrium time-dependent concentrations of premicellar aggregates, spherical and cylindrical micelles in relaxation far from equilibrium has been found. The existence of ultrafast relaxation and possibility of nonmonotonic behavior of the monomer concentration has been confirmed. Comparison with predictions of analytical kinetic theory of relaxation and micellization for concentration of monomers and total concentrations for spherical and cylindrical micelles has been given. It has been shown that the analytical theory is in fine agreement with the results of the difference Becker-Döring kinetic equations both for fast and slow nonlinear relaxation.

Introduction

Self-assembling of stable surfactant aggregates in micellar systems and relaxation of the ensembles of these aggregates to aggregative equilibrium are vivid examples of statistical behavior in complex systems initiated by the hydrophobic effect. Micelle formation, i.e. micellization, is a fundamental property of surfactants in solutions.[1-4] Understanding thermodynamic and kinetic regularities of micellization opens new possibilities for experimental study and applications of micellar systems. It gives a key to design of new detergents, solvents and nanoreactors.

In many aspects, micellization is similar to nucleation phenomena.[5] Its thermodynamics is governed by the work of aggregation as a function of the aggregation number, surfactant concentration and temperature in the surfactant solution. Its kinetics via the stepwise molecular mechanism can be described with the help of the Becker-Döring kinetic equations[6] initially proposed for nucleation kinetics. However the micelles are not the nuclei of a new phase. Their thermodynamic models, as well as the rates of attachment-detachment of monomers, are more complicated. With increasing the total surfactant concentration, micelles of new shapes and sizes appear. Thus, in addition to the spherical micelles observed above the first critical micelle concentration (cmc_1), cylindrical micelles are formed above the second critical micelle concentration (cmc_2).

While a number of works on molecular modeling of micellar systems via molecular dynamics and Monte Carlo methods increased significantly during last decades,[7,8] studies of self-aggregation kinetics via numerical approaches were relatively rare. One of the ways to address this problem is a stochastic simulation. A corresponding variant of Monte Carlo method, introduced by Gillespie[9] and employed by other groups for the studies of micellar systems,[10,11] gave a valuable information on micellization kinetics.

Mavelli and Maestro[10] adapted Gillespie's general method for stochastic simulations of surfactant solutions. Their model for micelle formation allowed fusion and fission of the aggregates with various aggregation numbers. A semi-empirical approach was used to determine kinetic constants. The results of the simulations appeared to be in good agreement with

Aniansson's kinetic theory[12,13] which was the first application of the Becker-Döring equations to kinetics of micellar systems.

Marrink *et al*[11] investigated aqueous solution of dodecylphosphocholine by molecular dynamics simulations. Diffusion coefficients of the aggregates, their sizes, and corresponding rate constants were obtained. Along with that, the results of the stochastic simulations carried out in Ref.[11] showed a discrepancy for the rate constants in comparison with the molecular dynamics data.

Micelle formation and disintegration are processes involving many time scales. A sophisticated model for treating these phenomena was proposed by Mohan and Kopelevich.[14] This model provided a link between stochastic description of micellar kinetics and underlying molecular mechanisms modeled by the molecular dynamics method. For a system of nonionic spherical micelles, the authors studied fast processes via the coarse-grained molecular dynamics. The attachment-detachment rates were obtained from the Brownian dynamics simulations with the assumption of the dominant stepwise mechanism of the aggregate formation. These rates were later used in the kinetic equations describing the aggregation. Thus, a multi-scale model for micellar kinetics was formulated.

A description and numerical investigation of the possible aggregation models, even beyond the stepwise mechanism, for surfactant solutions was given by Starov et al.[15] Four models denoted in Ref.[15] as A, B, C, and D were considered. According to A and B models, aggregation/disaggregation occurs symmetrically by attachment/detachment of single surfactant molecules (A) or clusters of arbitrary size (B). Models C and D describe an asymmetric mechanism: clusters of any size can associate but only single molecules can leave aggregates (C), or opposite (D). Analytical and numerical treatment of the kinetic equations showed[15] that C was the only model yielding a transition from the equilibrium distribution of the low sized clusters to the bimodal distribution of premicellar aggregates and micelles above the critical surfactant concentration.

Here we will be interested in results based on the approach with direct numerical solution of the difference Becker-Döring equations for non-equilibrium aggregate concentrations in the kinetics of micellization and relaxation. Initially this approach has been developed for spherical micelles.[12,13,16-25] In Refs.[26,27] the approach had been extended to the case of mixed and ionic spherical micelles. Last years the kinetic description in frameworks of the Becker-Döring equations has been extended to systems with cylindrical micelles and coexisting spherical and cylindrical micelles.[28-35]

We will focus in this paper on description of aggregation dynamics in a micellar solution with coexisting premicellar aggregates, spherical and cylindrical micelles at large initial deviations from the final equilibrium. The description is assumed to be a complete, i.e., to give a total behavior of the system since initial moment to establishing final equilibrium state. A similar approach has been recently applied by us to systems with spherical micelles[25] and systems with cylindrical micelles.[34] However, a kinetic behavior far from equilibrium in the systems with coexisting premicellar aggregates, spherical and cylindrical micelles has not yet been considered in the literature. As follows from the study of exponential relaxation at small deviations from final equilibrium,[35] there are several different time scales in such systems determining fast and slow processes. At large deviations from final equilibrium, one may expect an appearance of additional time scales as a result of considerable interplay between aggregates of different shapes and sizes in their consumption and emission of surfactant monomers. A question arises about the direct influence of initial conditions on the total kinetic behavior of micellar systems. It will be also of interest to compare the numerical results with the analytical ones for the nonlinear continuous Becker-Döring kinetic equation for such complex systems.[28,31,32]

The paper is organized as follows. The nonlinearized difference equations of stepwise aggregation with models for their coefficients are considered in Section 1. The time-dependent behavior of concentrations of aggregates with different aggregation numbers in three typical situations far from final equilibrium is analyzed in sections 2 - 4. In Section 2, the case of solutions with total surfactant concentration exceeding the cmc_2 and with zero initial concentrations of spherical and cylindrical micelles is considered. In this case we observe a proper micellization with formation of premicellar aggregates, stable spherical micelles and cylindrical micelles. Time evolution of aggregate concentrations in the course of relaxation in the case of substantial initial excess of surfactant monomers is present in section 3. The case of substantial initial deficit of surfactant monomers is considered in section 4. Sections 3 and 4 include also a comparison with predictions of analytic nonlinear kinetic theory of self-aggregation and relaxation. Conclusions are made in the last section.

1. Kinetic equations of self-aggregation

Kinetics of stepwise formation and fragmentation of aggregates with different aggregation numbers n, including monomers as a particular case of aggregates with $n=1$, is governed by the system of the Becker-Döring difference equations for non-equilibrium aggregate concentrations $c_n(t)$ as functions of time t.[5,6,21,23,24] For a closed system with fixed total surfactant concentration $C=\sum_{n=1}^{n_m} nc_n$ and finite upper aggregation number n_m, the Becker-Döring difference equations can be written as[25,34,35]

$$\frac{\partial c_1}{\partial t} = -\sum_{n=1}^{n_m-1}\left(a_n c_1 c_n - b_{n+1}c_{n+1}\right), \quad (1)$$

$$\frac{\partial c_2}{\partial t} = \frac{1}{2}a_1 c_1^2 - b_2 c_2 - a_2 c_1 c_2 + b_3 c_3, \quad (2)$$

$$\frac{\partial c_n}{\partial t} = a_{n-1}c_1 c_{n-1} - b_n c_n - a_n c_1 c_n + b_{n+1}c_{n+1}, \quad n=3,\ldots n_m. \quad (3)$$

Here a_n are the aggregate-monomer attachment coefficients, the aggregate-monomer detachment coefficients $b_{n+1} = a_n \frac{\tilde{c}_1 \tilde{c}_n}{\tilde{c}_{n+1}}$ are expressed via the detailed balance relations through a_n, the Boltzmann distribution $\tilde{c}_{n+1}$ and the monomer concentration $\tilde{c}_1$ in the state of final equilibrium of the micellar solution,

$$\tilde{c}_n = c_1 e^{-W_n} = c_1^n e^{-\overline{W}_n}. \quad (4)$$

We will distinguish the proper aggregation work W_n (free energy of aggregate formation expressed in thermal energy units $k_B T$ where k_B is the Boltzmann constant and T is the absolute temperature of solution) and the shifted aggregation work $\overline{W}_n = W_n + (n-1)\ln c_1$ which depends only on aggregation number n in the case of ideal mixture of aggregates. Here and below, the monomer concentration c_1 is assumed to be dimensionless and measured in units of the monomer concentration at which $W_n = \overline{W}_n$.

A micellar solution with coexisting premicellar aggregates, spherical and cylindrical micelles exists at the total surfactant concentration in the vicinity and above the cmc_2. A corresponding model equilibrium distribution $\tilde{c}_n$ had been previously considered in literature.[28,35-38] The aggregation work W_n at such total surfactant concentrations should have as a function of aggregation number two maxima at points $n_c^{(1)}$ and $n_c^{(2)}$, two minima at points $n_s^{(1)}$ and $n_s^{(2)}$ and slowly increasing linear tail at $n > n_0$. Such model function generalizes the models for the work W_n which we have recently used for separate kinetic modeling of spherical and cylindrical micelles.[33,34] Evidently, the values $n_c^{(1)}$, $n_c^{(2)}$, $n_s^{(1)}$, $n_s^{(2)}$, and n_0 depend on the surfactant monomer concentration. Taking parameters of the model in such way that monomer concentration $c_1 = 1$ corresponds to the total concentration in the vicinity of cmc_2, we propose

$$\overline{W}_n = \begin{cases} w_1(n-1)^{4/3} + w_2(n-1) + w_3(n-1)^{2/3}, & 1 \le n \le \bar{n}_s^{(1)}, \\ v_1(n-\bar{n}_s^{(1)})^4 + v_2(n-\bar{n}_s^{(1)})^3 + v_3(n-\bar{n}_s^{(1)})^2 + \overline{W}_s^{(1)}, & \bar{n}_s^{(1)} \le n \le \bar{n}_0, \\ \bar{k}(n-\bar{n}_0) + \overline{W}_0, & n > \bar{n}_0. \end{cases} \quad (5)$$

Here the values $\bar{n}_s^{(1)}, \bar{n}_s^{(2)}$, and $\bar{n}_0$ coincide with the values $n_s^{(1)}, n_s^{(2)}$, and n_0 at the monomer concentration $c_1 = 1$, $\overline{W}_s^{(1)}$ is the value of the first minimum of the work $\overline{W}_n$, $\overline{W}_0 \equiv \overline{W}_n\big|_{n=\bar{n}_0}$. It is assumed in eq.(3) that work $\overline{W}_n$ for aggregates with aggregation numbers $n \le \bar{n}_s^{(1)}$ corresponds to the simplified droplet model for spherical aggregates[25,39] with maximum at $\bar{n}_c^{(1)}$ and minimum at $\bar{n}_s^{(1)}$, while the work at $n > \bar{n}_0$ refers to the linear model[28,34,35] for cylindrical aggregates. In the transient (from spherical to cylindrical aggregates) range $\bar{n}_s^{(1)} < n, \bar{n}_0$, we use a polynomial interpolation having a maximum at $\bar{n}_c^{(2)}$ and two minima at $\bar{n}_s^{(1)}$ and $\bar{n}_s^{(2)}$. As the parameters of the work $\overline{W}_n$, we have fixed several characteristic points: the locations $\bar{n}_s^{(1)}$ and $\bar{n}_s^{(2)}$ of two minima of the work, the values $\overline{W}_s^{(1)}$ and $\overline{W}_s^{(2)}$ of these minima and the values $\overline{W}_c^{(1)}$ and $\overline{W}_c^{(2)}$ ($\overline{W}_c^{(1)} > \overline{W}_c^{(2)}$) of the maxima of the work (but not the locations of these maxima). These six conditions determine six parameters w_i and v_i ($i = 1,2,3$), while additional two conditions of continuity of function $\overline{W}_n$ and its derivative with respect to aggregation number at $n = \bar{n}_0$ at fixed $\bar{k}$ determine $\bar{n}_0$ and $\overline{W}_0$. Selection of the point of minimum $\bar{n}_s^{(1)}$ as a point of patching the droplet and transient models is convenient for finding the parameters of the aggregation work. However it has a major drawback because it does not ensure equality of second derivatives of the model functions at the minimum and makes asymmetric potential well even for small deviations from the minimum point. Nevertheless we can minimize the degree of this asymmetry and consider the following set of fixed parameters determining work $\overline{W}_n$:

$$\overline{W}_c^{(1)} = 15,\ \bar{n}_s^{(1)} = 100,\ \overline{W}_s^{(1)} = 5,$$
$$\overline{W}_c^{(2)} = 14,\ \bar{n}_s^{(2)} = 300,\ \overline{W}_s^{(2)} = 9,\ \bar{k} = 0.01. \quad (6)$$

As a consequence, other parameters entering eq.(5) are

$$\bar{n}_c^{(1)} = 16,\ \bar{n}_c^{(2)} = 211,\ w_1 = 0.4317,\ w_2 = -4.0955,$$
$$w_3 = 9.9403,\ v_1 = 6.8358 \cdot 10^{-8},\ v_2 = -2.8343 \cdot 10^{-5},$$
$$v_3 = 3.0343 \cdot 10^{-3},\ \bar{n}_0 = 301,\quad \overline{W}_0 = 9.0025. \quad (7)$$

It is possible to say that fixing the values of the aggregation work parameters we fix the properties of surfactant and solution. We chose these values as quite representative, for instance, for water solutions of nonionic surfactants of the alkyl poly(ethylene glycol) type.[40] The results of computations with the help of eqs.(1)-(3) are sensitive to these values as they should be sensitive to a specific surfactant. Shift in these values will change the values of cmc_1 and cmc_2.

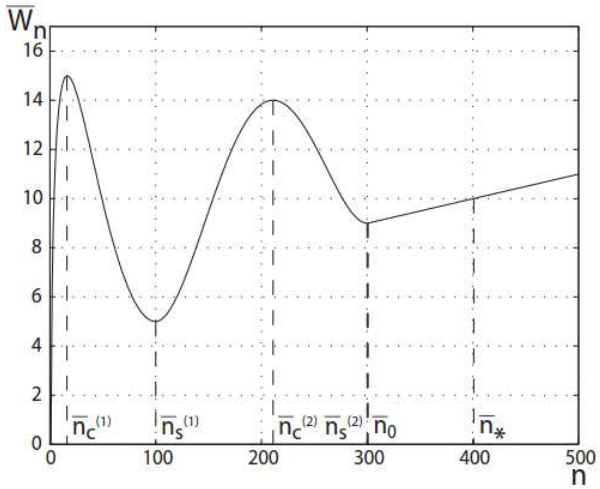

Fig.1 The micellization work $\overline{W}_n$ as a function of the aggregation number n.

The detailed behavior of work $\overline{W}_n$ as a function of aggregation number n is shown in Fig.1. The asymmetry of the work in the vicinity of minimum at $n = \bar{n}_s^{(1)}$ is small. Maximal value

n_m of the aggregation number for work $\overline{W}_n$ is $n_m = 3500$. This value was chosen to provide that the main part of surfactant (more than 99,97%) is gathered in equilibrium in aggregates with $1 \le n \le n_m$.

The equilibrium monomer concentration for the micellar system at cmc_2 can be determined from the condition that the total number of surfactant molecules in cylindrical micelles equals at equilibrium 10 percent of the total surfactant concentration. This condition can be written in the form

$$\sum_{n=n_c^{(2)}}^{n_m} n\tilde{c}_n \Big/ \sum_{n=1}^{n_m} n\tilde{c}_n = 0.1 \ . \qquad (8)$$

Solving eq.(8) after substituting eqs.(4)-(7) gives $(\tilde{c}_1)_{cmc_2} = 0.9977$.

The kinetic model for the aggregate-monomer attachment coefficients a_n should correspond to the model for the aggregation work $\overline{W}_n$ and be different for spherical aggregates at aggregation numbers $1 \le n \le \overline{n}_s^{(1)}$, for transient aggregates at aggregation numbers $\overline{n}_s^{(1)} \le n \le \overline{n}_0$, and for cylindrical aggregates at $n > \overline{n}_0$. Such a model has been considered in Refs.[34,35] Under assumption of the Brownian diffusion kinetics[41] for molecular aggregates and monomers in solution, attachments of monomers to a spherical aggregate occur with a stationary diffusion rate. This rate can be written as $a_n \propto (R_1 + R_n)(D_1 + D_n)$ where R_n and D_n represent the radius and the diffusion coefficient of aggregate $\{n\}$ in surfactant solution. With using the Stokes–Einstein formula for diffusivities of spherical aggregates, $D_n \propto 1/R_n$, and the droplet model for the dependence of aggregate radius on n in the form $R_n \propto n^{1/3}$, we have at $1 << n < n_c^{(2)}$: $a_n \propto n^{1/3}$.[25] At $n \ge \overline{n}_0$ the diffusivities of cylindrical micelles become small. Then it is sufficient for calculation of a_n to find the stationary flux of monomers onto immobile cylindrical body in polar coordinates. This flux will be proportional to the length of the cylindrical body. Since the radius of the body is fixed for cylindrical micelles, the length of the body itself is proportional to the aggregation number n. Thus we have $a_n \propto n$ at $n > \overline{n}_0$.[34] In view of the above consideration, we will use the following continuous model for the attachment coefficients a_n at arbitrary n:

$$a_n = \frac{n^{1/3}(n + \overline{n}_0)^{2/3}}{\overline{n}_0}, \quad 1 \le n \le n_m - 1, \ a_{n_m} = 0 . \qquad (9)$$

This formula matches the asymptotic cases for spherical aggregates at $n << \overline{n}_0$ and for cylindrical aggregates at $n >> \overline{n}_0$. It includes the specific factor coming from the proportionality constants as a scale into the quantity a_n. As is clear, the attachment coefficient a_n should have a dimensionality of reciprocal time. Representation of the quantity a_n in the form (9) means that we consider a dimensionless time.

In our study of initially large deviations of non-equilibrium state of the micellar system with coexisting premicellar aggregates, spherical and cylindrical micelles, the concentrations of aggregates at arbitrary moment of time t can be represented in view of eq.(4) as

$$c_n(t) = A_n(t) c_1^n(t) \exp(-\overline{W}_n) . \qquad (10)$$

Here the pre-exponential factor $A_n(t)$ tends to 1 and $c_1(t) \to \tilde{c}_1$ as $t \to \infty$. In view of eq.(10), the initial distribution of surfactant aggregates in solution is characterized as

$$c_n(0) = A_n(0) c_1^n(0) \exp(-\overline{W}_n) . \qquad (11)$$

As follows from eqs.(4) and (10), the pre-exponential factor $A_n(t)$ has a meaning of the aggregate distribution in aggregation number normalized to the quasi-equilibrium distribution at current monomer concentration $c_1(t)$. Deviation of quantity A_n from unity indicates a nonequilibrium state of micellar solution. If $A_n(t)$ appears to be independent on n in some range of aggregation numbers, the micellar system approaches a locally quasi-equilibrium state in this range.

2. Micellization at initial zero concentrations of aggregates with $n > 1$

First we will consider dynamics of micellization, i.e., transition in the surfactant solution to final equilibrium at total surfactant concentration above the cmc_2 in the situation when initially the solution contains only surfactant monomers. Thus we set

$$A_n(0) = \delta_{1n} \qquad (12)$$

in eq.(11) for the distribution $c_n(0)$ which serves as initial condition for eqs.(1)-(3).

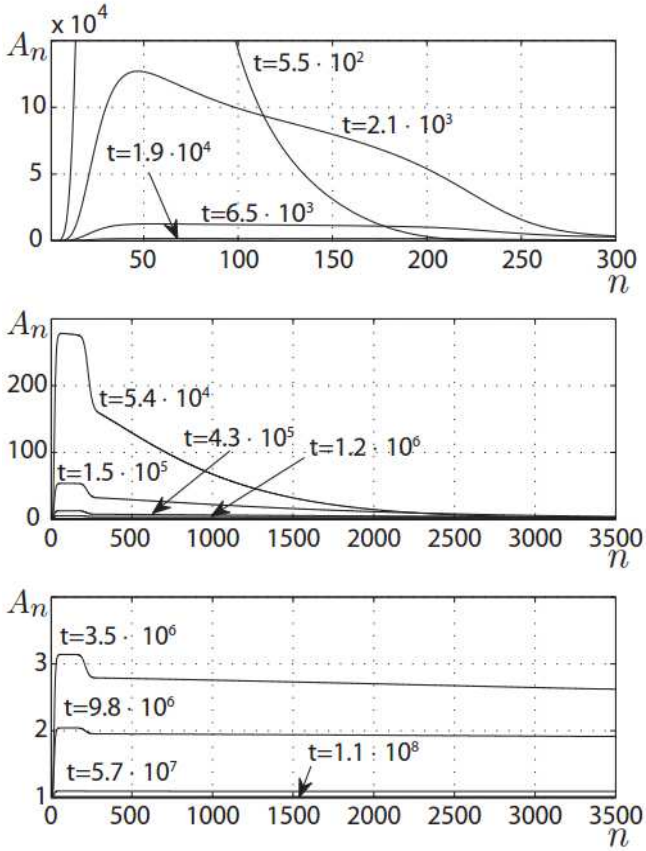

Fig.2 Normalized aggregate distribution $A_n(t)$ at different stages of micellization at $c_1(0) = 73.474$ and $\tilde{c}_1 = 1.004$.

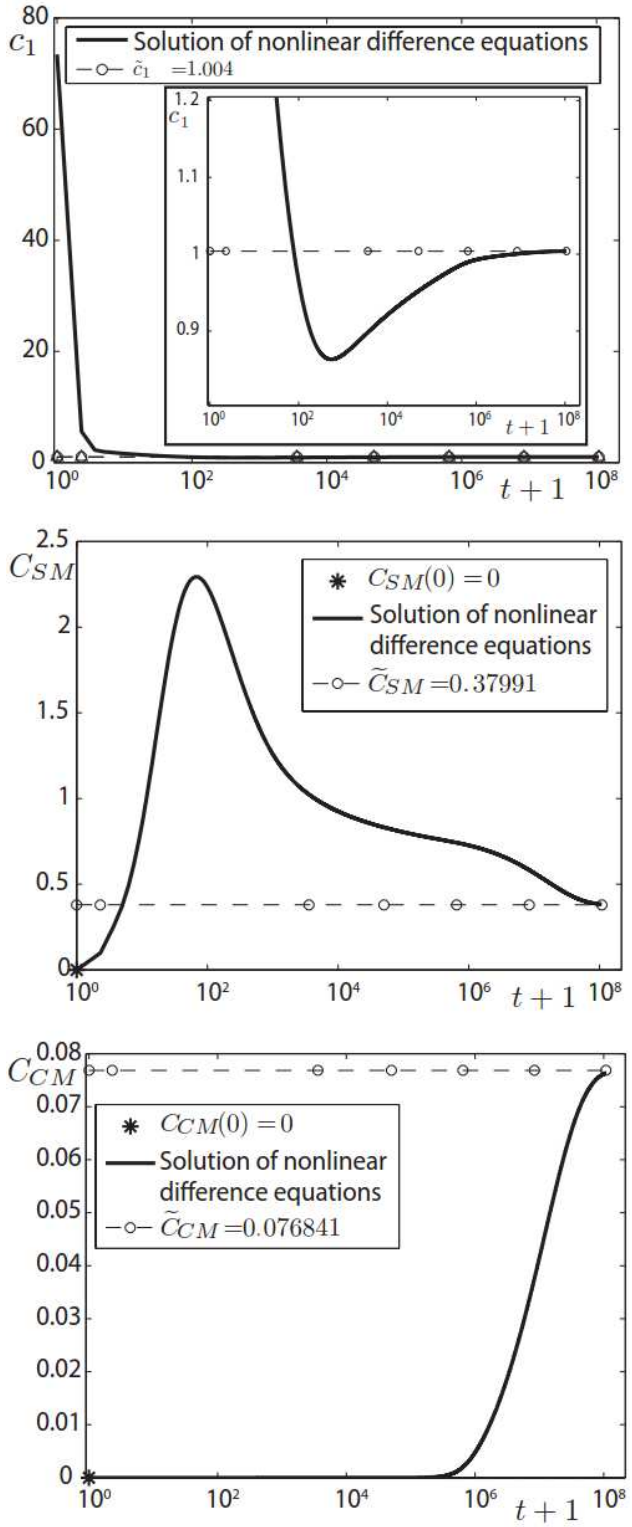

Fig.3 The monomer concentration $c_1(t)$, the total concentration $C_{SM}(t)$ of spherical micelles and the total concentration $C_{CM}(t)$ of cylindrical micelles at different stages of micellization at $c_1(0)=73.474$ and $\tilde{c}_1=1.004$.

Solving eqs. (1)-(3) simultaneously with initial condition (12) and the coefficients a_n determined according to eqs.(4)-(7),(9) at $c_1(0)=73.474$ and $\tilde{c}_1=1.004$ ($\tilde{c}_1>(\tilde{c}_1)_{cmc_2}=0.9977$), we have computed aggregate concentrations $c_n(t)$ as functions of time at any aggregation number n. The corresponding behavior of the normalized aggregate distribution $A_n(t)$ at different time scales is shown in Fig.2.

In addition, the whole picture of micellization and its stages can be illustrated by dependences on time of the monomer concentration $c_1(t)$, total concentration $C_{SM}(t)\equiv\sum_{n\in\{SM\}}c_n(t)$ of spherical and total concentration $C_{CM}(t)\equiv\sum_{n\in\{CM\}}c_n(t)$ of cylindrical micelles shown in Fig.3. The range $\{SM\}$ of aggregation numbers for spherical micelles lies in the vicinity of first maximum of the aggregate distribution, while the range $\{CM\}$ of aggregation numbers for cylindrical micelles extends from the vicinity of second maximum of the aggregate distribution to number n_m. For quasi-equilibrium and equilibrium states we can write $\{SM\}=\left(n_c^{(1)},n_c^{(2)}\right)$ and $\{CM\}=(n_c^{(2)},n_m]$.

The large concentration of monomers at the beginning of micellization provides that initial value of $n_c^{(1)}$ is very small. As a result, the activation barrier for passing from monomers to spherical micelles is low.[5,21] All of this enables a very fast and intensive formation of spherical aggregates with consumption of monomers until the monomer concentration drops from $c_1(0)=73.474$ to its intermediate value $c_1\approx1.2$. It occurs to the moment of time $t\approx70$. In Fig.3, the total concentration of spherical micelles reaches its maximal value $C_{SM}=2.2939$ to the same moment of time. After that to the moment of time $t\approx3\cdot10^2$, the monomer concentration continues to decrease to its minimal value $c_1=0.8631$, lying considerably below the final value $\tilde{c}_1=1.004$. Thus the monomer concentration $c_1(t)$ and the total concentration $C_{SM}(t)$ of spherical aggregates demonstrate a nonmonotonic time behavior. There is no visible change in total concentration of cylindrical aggregates of such times.

The nonmonotonic behavior of the total concentration of the spherical micelles and the monomer concentration can be commented in the following way. With decreasing the monomer concentration during the initial stage, the current value of $n_c^{(1)}$ and the activation barrier for passing from monomers and premicellar aggregates to spherical micelles grow. As a result, a number of stable spherical aggregates which have been formed from the very beginning turn back to be premicellar aggregates. The number of cylindrical micelles stays to be very small at this stage. For times larger than $t\approx3\cdot10^2$ but less than $t\approx6.5\cdot10^3$, we observe in the first slides of Figs.2 and 3 an increase of the monomer concentration due to detachment of monomers from premicellar and micellar aggregates and a decrease of the total concentration of aggregates, especially with small aggregation numbers. Larger aggregates grow due to disintegration of smaller premicellar aggregates. At the same time, the normalized aggregate distribution $A_n(t)$ tends to be independent of aggregation number n in the region of spherical micelles, and this means establishing a local equilibrium in

this region. Still there is only a small number of cylindrical micelles on this stage of micellization. As follows from the second slide in Fig.2, the number of cylindrical micelles becomes significant on time scale $\Delta t \approx 10^5$, and up to the moment of time $t \approx 4.3 \cdot 10^5$ we observe approaching $A_n(t)$ to a horizontal line in the region of cylindrical micelles, i.e., establishing the local equilibrium in this region.

Since the horizontal linear parts of $A_n(t)$ are different in the regions for spherical and cylindrical micelles on the third slide in Fig.2, the local aggregate equilibriums for these micelles are also different and merge only to moment of time $t \approx 6 \cdot 10^7$. It is not a complete equilibrium, because the equilibrium of micelles with monomers and premicellar aggregates is not yet reached. The complete equilibrium is achieved at times $t > 10^8$ when equality $A_n(t) = 1$ holds everywhere.

3. Relaxation at large initial excess of monomers

Let us now turn to the case of large initial excess of surfactant monomers in comparison to the equilibrium concentration of monomers. Spherical and cylindrical aggregates are also present at the initial moment of time.

We determine initial distribution of aggregates in the aggregation number in the form

$$c_n(0) = \tilde{c}_n (1+\eta)^{-W_n(\tilde{c}_1)} \frac{\sum_{k=1}^{n_m} k\tilde{c}_k}{\sum_{l=1}^{n_m} l\tilde{c}_l (1+\eta)^{-W_l(\tilde{c}_1)}}. \qquad (13)$$

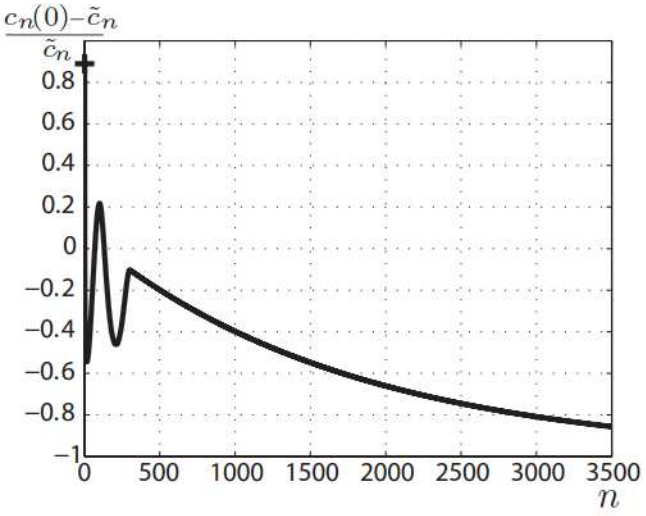

Fig.4 Initial aggregate distribution $\left(c_n(0) - \tilde{c}_n\right)/\tilde{c}_n$ in aggregation number at $\eta = 0.1$ and $\tilde{c}_1 = 1.004$ ($c_1(0) = 1.8971$).

Here η is a perturbing parameter and $\tilde{c}_n$ is the equilibrium distribution (4) of the aggregates at the same temperature and total surfactant concentration as for unperturbed system. Last factor with the ratio of sums in eq.(13) ensures that the total surfactant concentration C satisfies equality $C = \sum_{n=1}^{n_m} n\tilde{c}_n = \sum_{n=1}^{n_m} n c_n(0)$. At $\eta = 0$ there is no disturbance, and $c_n(0) = \tilde{c}_n$. At $\eta = 0.1$ and $\tilde{c}_1 = 1.004$ (this monomer concentration corresponds to $C = 73.474$) it follows from eq.(13) that $c_1(0) = 1.8971$. This allows us to choose the value $\eta = 0.1$ as providing a large initial excess of surfactant monomers. At $\eta = 0.1$ the relative deviation of the aggregate concentrations $\left(c_n(0) - \tilde{c}_n\right)/\tilde{c}_n$ has the form shown in Fig.4.

In view of eqs.(4), (11) and (13), the initial value of the pre-exponential factor $A_n(t)$ in eq. (10) can be written now as

$$A_n(0) = \left[\frac{\tilde{c}_1}{c_1(0)}\right]^n (1+\eta)^{-W_n(\tilde{c}_1)} \frac{\sum_{k=1}^{n_m} k\tilde{c}_k}{\sum_{l=1}^{n_m} l\tilde{c}_l (1+\eta)^{-W_l(\tilde{c}_1)}}. \qquad (14)$$

Solving numerically eqs.(1)-(3) with initial condition (13) at $\eta = 0.1$ and the coefficients defined according to eqs.(4)-(7),(9) at $c_1(0) = 1.8971$ and $\tilde{c}_1 = 1.004$ (thus $\tilde{c}_1 > (\tilde{c}_1)_{cmc_2} = 0.9977$), we have found the relaxation behavior of the normalized aggregate distribution $A_n(t)$ at different times as shown in Fig.5.

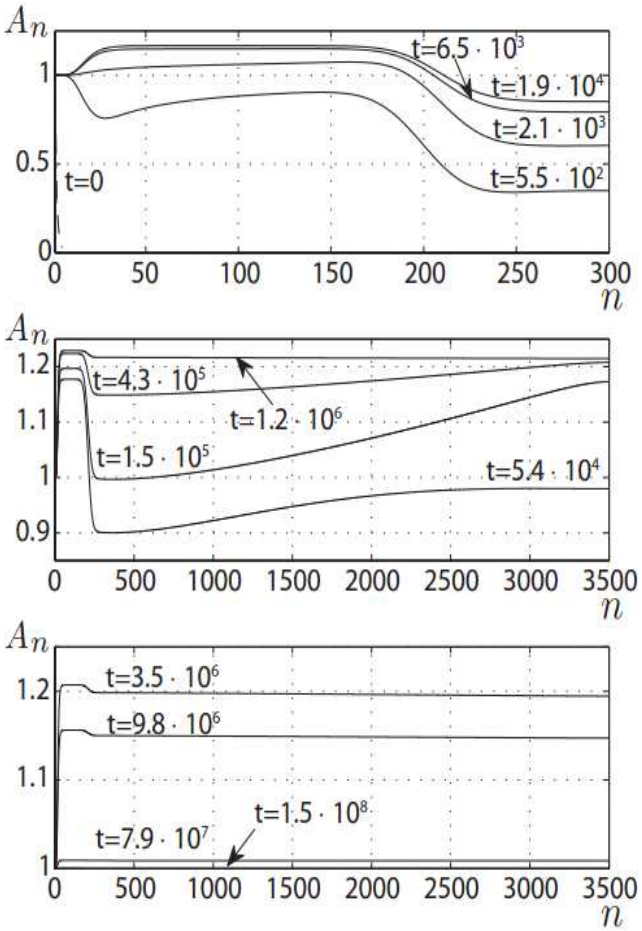

Fig.5 Normalized aggregate distribution $A_n(t)$ at different stages of relaxation at $\eta = 0.1$ and $\tilde{c}_1 = 1.004$ ($c_1(0) = 1.8971$).

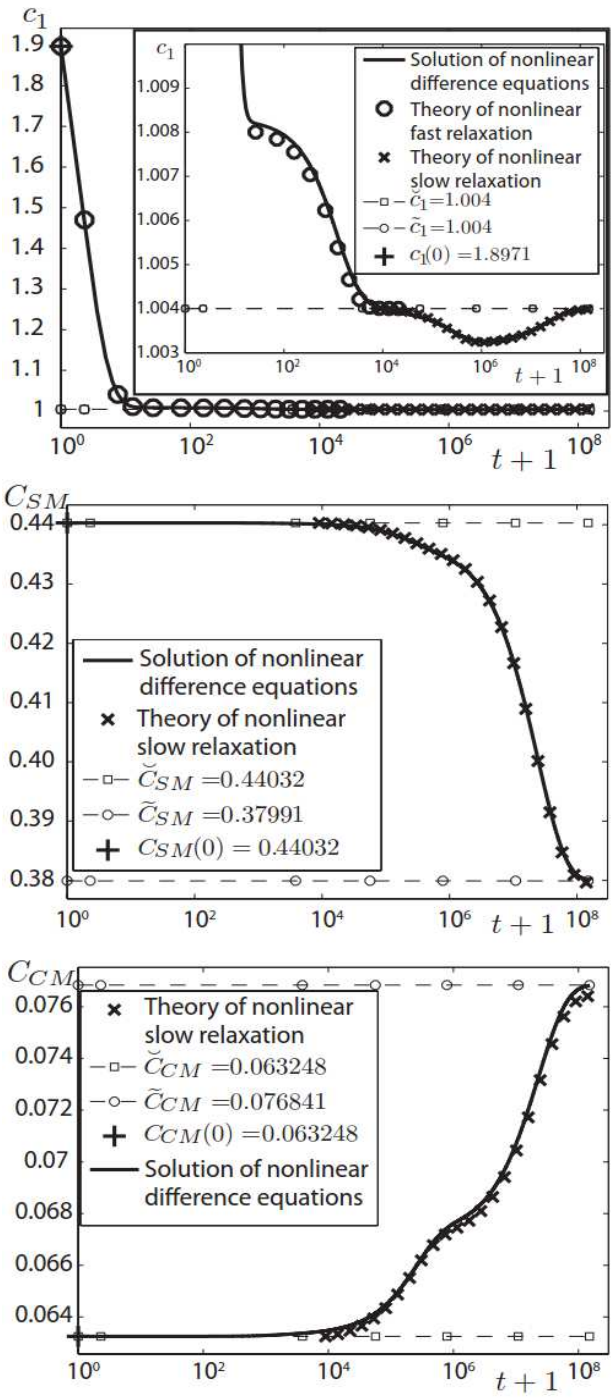

Fig.6 The monomer concentration $c_1(t)$, the total concentration $C_{SM}(t)$ of spherical micelles and the total concentration $C_{CM}(t)$ of cylindrical micelles at different stages of relaxation at $\eta = 0.1$ and $\tilde{c}_1 = 1.004$.

As follows from the first slide in Fig.5, function $A_n(t)$ becomes independent on n in the range $n = 1 \div 10$ to the moment of time $t = 5.5 \cdot 10^2$. Thus the quasi-equilibrium distribution of premicellar aggregates establishes very fast. Then, to the moment of time $t = 2.1 \cdot 10^3$, we can observe establishing a quasi-equilibrium state for spherical aggregates within range $n = 30 \div 170$. Almost the same time is required for establishing the quasi-equilibrium state of smallest cylindrical micelles within the range $n = 230 \div 500$. With increasing the time, the states of the aggregate distribution in these ranges of aggregation number stay to be quasi-equilibrium. However the total numbers of spherical and cylindrical micelles change due to transitions over potential peak of the aggregation work between spherical and cylindrical aggregates. These transitions cause displacement of the local horizontal linear parts of distribution $A_n(t)$ in a vertical direction.

The second slide in Fig.5 shows that the micellar system on the next stage of evolution tends to establishing of local quasi-equilibrium in the whole range of aggregation numbers for cylindrical micelles, $n = 230 \div 3500$. This stage ends to the moment of time $t = 1.2 \cdot 10^6$.

The final stage of micellar relaxation is shown in the third slide in Fig.5. We observe here two different linear parts of function $A_n(t)$ decreasing to the moment of time $t = 7.9 \cdot 10^7$ to the join value. These parts relate to the quasi-equilibrium distributions of spherical and cylindrical micelles, respectively. The join plato for spherical and cylindrical micelles merges in the final equilibrium distribution with concentrations of monomers and premicellar aggregates to moment of time $t = 1.5 \cdot 10^8$.

To make more clear the whole picture of evolution of the micellar system with coexisting spherical and cylindrical micelles at large initial excess of surfactant monomers, let us analyze in addition the dependences on time for the monomer concentration $c_1(t)$, total concentration $C_{SM}(t)$ of spherical and total concentration $C_{CM}(t)$ of cylindrical micelles. These dependences follow from the computations of separate aggregate concentrations $c_n(t)$ and are shown in Fig.6.

As is seen from Figs.5 and 6, establishing the quasi-equilibrium distribution of premicellar aggregates to the moment of time $t = 5.5 \cdot 10^2$ is accompanied by the rapid drop of the surfactant monomer concentration from $c_1(0) = 1.8971$ to $c_1 = 1.0082$. Subsequent decrease in the monomer concentration is slower. At the value $\breve{c}_1 = 1.004$ which practically coincides with the final equilibrium value $\tilde{c}_1$, establishing a quasi-equilibrium state for spherical aggregates within range $n = 30 \div 170$ occurs to the moment of time $t = 2.1 \cdot 10^3$. On larger time scale, we observe further slow drop of the monomer concentration below its equilibrium value and then slow growth back to the equilibrium value. Thus the total behavior of the monomer concentration $c_1(t)$ turns to be non-monotonic. We observed a similar behavior of the monomer concentration in the previous section when considered micellization at initial zero concentrations of spherical and cylindrical micelles. Such similarity in the results for the monomer concentration is not surprising. The micellar system in presence of large aggregates with high aggregate-monomer attachment rate $a_n c_1$ and detachment rate $b_{n+1} = a_n \tilde{c}_1 \tilde{c}_n / \tilde{c}_{n+1}$ becomes an inert one. By contrast, the time behavior of total concentrations of spherical micelles $C_{SM}(t)$ and $C_{CM}(t)$ appear to be monotonic in the considered case, $C_{SM}(t)$ drops from

$C_{SM}(0)=0.44032$ to $\tilde{C}_{SM}=0.37991$ while $C_{CM}(t)$ grows from $C_{CM}(0)=0.063248$ to $\tilde{C}_{SM}=0.076841$. It is seen from Fig.6, that there is no change in the concentrations $C_{SM}(t)$ and $C_{CM}(t)$ until the moment of time $t=1\div 2\cdot 10^4$. This allows us to consider the corresponding stage of micellar relaxation as the fast relaxation stage.[12,13,30-32] It is not characterized by pure exponential dependence on time, and the deviations of the monomer concentration from its quasi-equilibrium value $\breve{c}_1$ on this stage are nonlinear. Another stage when the total concentrations $C_{SM}(t)$ and $C_{CM}(t)$ slowly approach their values at final equilibrium can be called a slow relaxation stage.[28,32] It is also the stage with nonlinear deviations of the monomer and micellar concentrations from their final equilibrium values, which demonstrates non-exponential behavior.

One of the goals of this study is to compare the numerical results obtained from the difference Becker-Döring equations for nonlinear micellar relaxation in solutions of coexisting spherical and cylindrical micelles with the analytical ones. An analytical theory for fast and slow relaxation in such complex systems was built on the basis of the continuous Becker-Döring kinetic equation.[28,31,32]

The set of two coupled equations had been derived in Ref.[31] for evolution of coexisting spherical and cylindrical micelles on the stage of fast relaxation. In our notation, it can be rewritten as

$$\frac{d}{dt}\Delta M_1^{SM}=-\breve{a}_{\breve{n}_{SM}}\breve{c}_1\left[\left(\frac{\breve{C}_{SM}}{\breve{c}_1}+\frac{2}{\left(\Delta\breve{n}_{SM}\right)^2}\right)\Delta M_1^{SM}+\frac{\breve{C}_{SM}}{\breve{c}_1}\Delta M_1^{CM}\right], \quad (15)$$

$$\frac{d}{dt}\Delta M_1^{CM}=-\frac{\breve{a}_{\breve{n}_{CM}}\breve{c}_1}{\breve{n}_{CM}}\left[\left(\frac{\breve{C}_{CM}\breve{n}_{CM}}{\breve{c}_1}+\frac{1}{\Delta\breve{n}_{CM}}\right)\Delta M_1^{CM}+\right.$$

$$\left.+\frac{\breve{C}_{CM}\breve{n}_{CM}}{\breve{c}_1}\Delta M_1^{SM}+\left(\Delta M_1^{SM}+\Delta M_1^{CM}\right)\Delta M_1^{CM}\right], \quad (16)$$

where

$$\Delta M_1^{SM}(t)\equiv\frac{1}{\breve{c}_1}\sum_{n\in\{SM\}}n\left[c_n(t)-\breve{c}_n\right], \quad (17)$$

$$\Delta M_1^{CM}(t)\equiv\frac{1}{\breve{c}_1}\sum_{n\in\{CM\}}n\left[c_n(t)-\breve{c}_n\right], \quad (18)$$

$$\breve{n}_{SM}\equiv\frac{1}{\breve{C}_{SM}}\sum_{n=\breve{n}_c^{(1)}}^{\breve{n}_c^{(2)}}\breve{c}_n n, \quad \left(\Delta\breve{n}_{SM}\right)^2\equiv\frac{1}{\breve{C}_{SM}}\sum_{n=\breve{n}_c^{(1)}}^{\breve{n}_c^{(2)}}\breve{c}_n\left(n-\breve{n}_{SM}\right)^2, \quad (19)$$

$$\breve{n}_{CM}\equiv\frac{1}{\breve{C}_{CM}}\sum_{n=\breve{n}_c^{(2)}}^{n_m}\breve{c}_n n, \quad \left(\Delta\breve{n}_{CM}\right)^2\equiv\frac{1}{\breve{C}_{CM}}\sum_{n=\breve{n}_c^{(2)}}^{n_m}\breve{c}_n\left(n-\breve{n}_{CM}\right)^2. \quad (20)$$

It follows from the condition of surfactant matter balance $C=\sum_{n=1}^{n_m}nc_n=\sum_{n=1}^{n_m}n\breve{c}_n$ that the quantities $\Delta M_1^{SM}(t)$ and $\Delta M_1^{CM}(t)$ are related to the monomer concentration $c_1(t)$ as

$$\frac{c_1(t)-\breve{c}_1}{\breve{c}_1}=-\Delta M_1^{SM}(t)-\Delta M_1^{CM}(t). \quad (21)$$

Simultaneous solving eqs. (15), (16) with initial conditions

$$\Delta M_1^{SM}(0)=\frac{C_{SM}(0)}{\breve{c}_1}\left[n_{SM}(0)-\breve{n}_{SM}\right], \quad C_{SM}(0)=\breve{C}_{SM}, \quad (22)$$

$$\Delta M_1^{CM}(0)=\frac{C_{CM}(0)}{\breve{c}_1}\left[n_{CM}(0)-\breve{n}_{CM}\right], \quad C_{CM}(0)=\breve{C}_{CM}, \quad (23)$$

and substituting the result on the right-hand side of eq. (21) gives the function $c_1(t)$ shown in the first slide in Fig.6 by hollow circles. As is seen, the curves for the monomer concentration obtained by two approaches coincide for the stage of nonlinear fast relaxation.

In the case of nonlinear slow relaxation, we will use the formulation of the analytical theory done in Refs.[28,32] In our notation, we have the following three equations describing the slow evolution of the monomer concentration $c_1(t)$ and the total concentrations of spherical micelles $C_{SM}(t)$ and cylindrical micelles $C_{CM}(t)$:

$$\frac{dC_{SM}}{dt}=J_1'-J_1''-\left(J_2'-J_2''\right), \quad (24)$$

$$\frac{dC_{CM}}{dt}=J_2'-J_2'', \quad (25)$$

$$\frac{dc_1}{dt}=-\frac{n_{SM}\,dC_{SM}/dt+n_{CM}\,dC_{CM}/dt}{1+\left(\Delta n_{SM}\right)^2C_{SM}/c_1+\left(\Delta n_{CM}\right)^2C_{CM}/c_1}, \quad (26)$$

where J_1' and J_2' are the quasi-steady direct fluxes of aggregates over the first and second potential peaks of the aggregation work as a function of aggregation number, and J_1'' and J_2'' are the corresponding backward fluxes. These fluxes can be determined as

$$J_1'=a_{n_c^{(1)}}c_1^2\frac{\exp\left(-W_c^{(1)}\right)}{\pi^{1/2}\Delta n_c^{(1)}}, \quad (27)$$

$$J_1''=a_{n_c^{(1)}}c_1C_{SM}\frac{\exp\left(-W_c^{(1)}\right)}{\pi^{1/2}\Delta n_c^{(1)}}\frac{1}{\sum_{n\in\{SM\}}\exp\left(-W_n\right)}, \quad (28)$$

$$J_2'=a_{n_c^{(2)}}c_1C_{SM}\frac{\exp\left(-W_c^{(2)}\right)}{\pi^{1/2}\Delta n_c^{(2)}}\frac{1}{\sum_{n\in\{SM\}}\exp\left(-W_n\right)}, \quad (29)$$

$$J_2''=a_{n_c^{(2)}}c_1C_{CM}\frac{\exp\left(-W_c^{(2)}\right)}{\pi^{1/2}\Delta n_c^{(2)}}\frac{1}{\sum_{n\in\{CM\}}\exp\left(-W_n\right)}, \quad (30)$$

$$n_{SM}\equiv\frac{1}{C_{SM}}\sum_{n\in\{SM\}}c_n n, \quad \left(\Delta n_{SM}\right)^2\equiv\frac{1}{C_{SM}}\sum_{n\in\{SM\}}c_n\left(n-n_{SM}\right)^2, \quad (31)$$

$$n_{CM}\equiv\frac{1}{C_{CM}}\sum_{n\in\{CM\}}c_n n, \quad \left(\Delta n_{CM}\right)^2\equiv\frac{1}{C_{CM}}\sum_{n\in\{CM\}}c_n\left(n-n_{CM}\right)^2, \quad (32)$$

$$\left(\Delta n_c^{(1)}\right)^2 \equiv \frac{2}{\left|W_n''\right|_{n=n_c^{(1)}}}, \qquad \left(\Delta n_c^{(2)}\right)^2 \equiv \frac{2}{\left|W_n''\right|_{n=n_c^{(2)}}}. \tag{33}$$

The definitions of fluxes in eqs.(28)-(30) slightly differ from those in Refs.[28,32] by last factors. Instead of using the Gauss approximation for the aggregation work in the vicinity of the first potential well of the work and the Poisson approximation for the aggregation work for cylindrical aggregates at $n > n_c^{(2)}$, we have used here the formula $W_n = \bar{W}_n - (n-1)\ln c_1$ with work $\bar{W}_n$ determined by eq.(5).

Simultaneous solving eqs. (24)-(26) with initial conditions

$$c_1(0) = \breve{c}_1, \quad C_{SM}(0) = \breve{C}_{SM}, \quad C_{CM}(0) = \breve{C}_{CM} \tag{34}$$

gives the functions $c_1(t)$, $C_{SM}(t)$ and $C_{CM}(t)$ shown in Fig.6 by symbols $\times$. As is seen, the curves for these concentrations obtained by the solution of the difference Becker-Döring equations and by solution of eqs. (24)-(26) are in a fine agreement for the stage of nonlinear slow relaxation at initial excess of surfactant monomers.

4. Relaxation at large initial excess of surfactant matter in aggregates

By contrast to the linear deviations, relaxation at nonlinear deviations from the final state reveals different behavior with changing the sign of initial deviation. Let us now consider the situation of large initial deficit of surfactant monomers in comparison to the final equilibrium state of the micellar system with coexisting spherical and cylindrical aggregates. This situation is opposite to the case analyzed in the previous section.

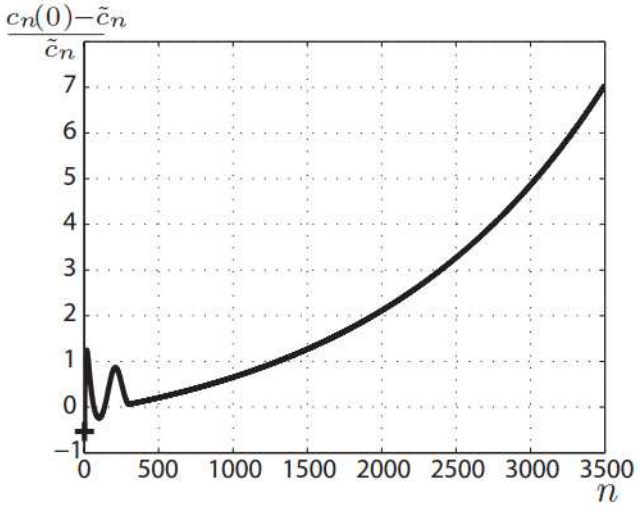

Fig.7 Initial aggregate distribution $\left(c_n(0)-\tilde{c}_n\right)/\tilde{c}_n$ in aggregation number at $\eta = -0.1$ and $\tilde{c}_1 = 1.004$ ($c_1(0) = 0.46853$).

We still can set initial distribution of aggregates in the aggregation number in the form of eq.(13). We provide $c_1(0) < \tilde{c}_1$ in eq.(13) if we take negative values of the perturbing parameter η. At $\eta = -0.1$ and $\tilde{c}_1 = 1.004$ ($C = 73.474$) it follows from eq.(13) that $c_1(0) = 0.46853$.

At $\eta = -0.1$ the relative deviation of the aggregate concentrations $\left(c_n(0)-\tilde{c}_n\right)/\tilde{c}_n$ has the form shown in Fig.7.

Solving numerically eqs.(1)-(3) with initial condition (13) at $\eta = -0.1$ and the coefficients defined according to eqs.(4)-(7),(9) at $c_1(0) = 0.46853$ and $\tilde{c}_1 = 1.004$ ($\tilde{c}_1 > (\tilde{c}_1)_{cmc_2} = 0.9977$), we have found the relaxation behavior of the normalized aggregate distribution $A_n(t)$ at different times as shown in Fig.8.

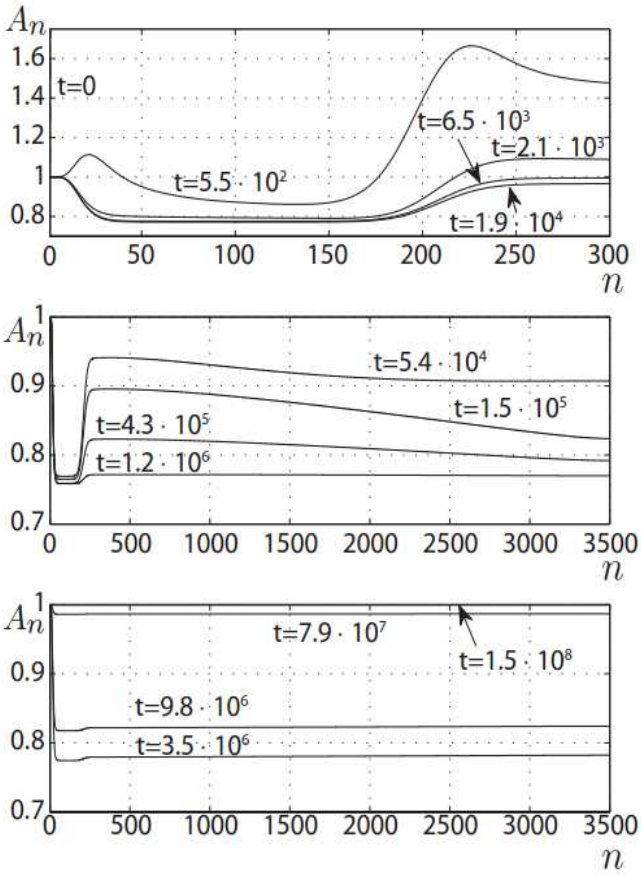

Fig.8 Normalized aggregate distribution $A_n(t)$ in aggregation number at different stages of relaxation at $\eta = -0.1$ and $\tilde{c}_1 = 1.004$ ($c_1(0) = 0.46853$).

As follows from the first slide in Fig.8, the quasi-equilibrium distribution of premicellar aggregates in the range $n = 1 \div 10$ establishes to the moment of time $t = 5.5 \cdot 10^2$. This ultrafast stage has been revealed also in the case of initial excess of monomers in Fig.5. As in Fig.5, establishing a quasi-equilibrium state for spherical aggregates within range $n = 30 \div 170$ is observed to the moment of time $t = 2.1 \cdot 10^3$. The same time is required for the establishing of the quasi-equilibrium state for the smallest cylindrical micelles in the range $n = 230 \div 500$. With increasing the time, the quasi-equilibrium states of the aggregate distribution in these ranges of aggregation number related to the local horizontal linear

parts of function $A_n(t)$ stay to be quasi-equilibrium. Again, as in Fig.5, total numbers of spherical and cylindrical micelles change due to transitions over potential peak of the aggregation work between spherical and cylindrical aggregates.

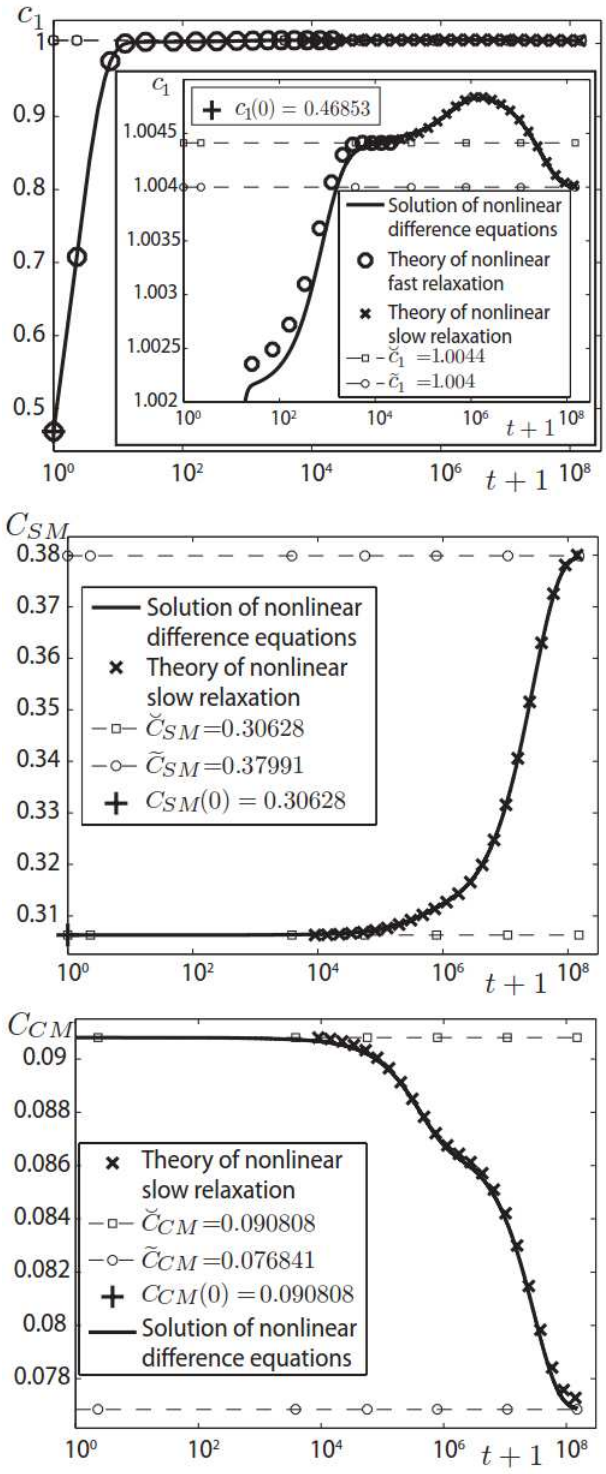

Fig.9 The monomer concentration $c_1(t)$, the total concentration $C_{SM}(t)$ of spherical micelles and the total concentration $C_{CM}(t)$ of cylindrical micelles at different stages of relaxation at $\eta = -0.1$ and $\tilde{c}_1 = 1.004$.

The second slide in Fig.8 shows that the micellar system tends on the next stage of evolution to establishing of local quasi-equilibrium in the whole range of aggregation numbers for cylindrical micelles, $n = 230 \div 3500$. This stage ends to the moment of time $t = 1.2 \cdot 10^6$. The time scales are the same as for the second slide in Fig.5 although the displacement of the curves with time is opposite.

The final stage of micellar relaxation is shown in the third slide in Fig.8. We observe here two different linear parts of function $A_n(t)$ which rise with the growth of time to the value 1. These parts relate to the quasi-equilibrium distributions of spherical and cylindrical micelles, respectively. They first form a joined quasi-equilibrium distribution to the moment of time $t = 7.9 \cdot 10^7$ and then merge to the moment of time $t = 1.5 \cdot 10^8$ in the final equilibrium distribution with concentrations of monomers and premicellar aggregates. Again, these time scales coincide with those in Fig.5.

Let us now analyze in addition the dependences on time for the monomer concentration $c_1(t)$, total concentration $C_{SM}(t)$ of spherical and total concentration $C_{CM}(t)$ of cylindrical micelles. These dependences follow from the computations for separate aggregate concentrations $c_n(t)$ and are shown in Fig.9.

As is seen from Figs.8 and 9, establishing the quasi-equilibrium distribution of premicellar aggregates to the moment of time $t = 5.5 \cdot 10^2$ is accompanied by the rapid rise of the surfactant monomer concentration from $c_1(0) = 0.46853$ to $c_1 = 1.0022$. Then the growth of monomer concentration becomes slower. The monomer concentration reaches the value $\breve{c}_1 = 1.0044$ (which is larger than the final equilibrium value $\tilde{c}_1 = 1.004$) to the moment of time $t = 2.1 \cdot 10^3$ when establishing a quasi-equilibrium state for spherical aggregates within range $n = 30 \div 170$ appears. The growth of the monomer concentration continues even further until maximal value $c_1 = 1.0048$ is reached at the moment of time $t = 1.2 \cdot 10^6$. To that moment, a local quasi-equilibrium in the whole range of aggregation numbers for cylindrical micelles is established. Subsequent monotonic slow decay of the monomer concentration to the final equilibrium value $\tilde{c}_1 = 1.004$ occurs until the moment of time $t = 1.5 \cdot 10^8$. Thus the total behavior of the monomer concentration $c_1(t)$ turns to be non-monotonic. By contrast, the time behavior of total concentrations of spherical micelles $C_{SM}(t)$ and $C_{CM}(t)$ appear to be monotonic, $C_{SM}(t)$ grows from $C_{SM}(0) = 0.30628$ to $\tilde{C}_{SM} = 0.37991$ while $C_{CM}(t)$ drops from $C_{CM}(0) = 0.090808$ to $\tilde{C}_{SM} = 0.076841$. It is seen from Fig.9, that there is no change in the concentrations $C_{SM}(t)$ and $C_{CM}(t)$ until the moment of time $t = 10^4$. Thus we confirm existence of the nonlinear fast and slow relaxation stage at initial deficit of monomers is the system with coexisting spherical and cylindrical micelles. Existence of the inflection points in curves for monomer concentration and total concentration of cylindrical micelles demonstrate general non-exponential behavior of these concentrations as functions of time at fast and slow relaxation.

Simultaneous solving eqs. (15), (16) with initial conditions (22) and (23) and eqs. (24)-(26) with initial conditions (34) at $\eta = -0.1$ and $\tilde{c}_1 = 1.004$ gives the function $c_1(t)$ shown in the first slide in Fig.8 by hollow circles and the functions $c_1(t), C_{SM}(t)$ and $C_{CM}(t)$ shown in the in Fig.9 by symbols $\times$. As is seen, the curves for these concentrations obtained by the solution of the difference Becker-Döring equations and by solution of eqs. (22), (23) and (24)-(26) are in a fine agreement for the stages of nonlinear fast and slow relaxation at initial deficit of monomers.

Conclusions

Our results for kinetic modeling of self-aggregation in surfactant solution with coexisting spherical and cylindrical micelles show the total behavior of all aggregate concentrations as functions of time at arbitrary initial conditions. We have considered the case of proper micellization with formation of premicellar aggregates, stable spherical micelles and cylindrical micelles, and the cases of micellar relaxation in such systems at large initial excess and deficit of surfactant monomers in solution over their equilibrium concentration. In all cases, we observed a stage of ultrafast relaxation at which concentration of surfactant monomers changes rapidly together with concentration of premicellar aggregates. A similar behavior was noted previously for systems with cylindrical micelles.[34] The stages of fast and slow relaxation are characterized by non-monotonic dependence on time for the monomer concentration. In the case of micellization, also the behavior of total concentration of spherical micelles is non-monotonic in time.

We have shown that the stages of fast and slow relaxation in solution with coexisting spherical and cylindrical micelles at arbitrary initial conditions include substages. It is possible to clarify the physical processes on these substages as corresponding to different quasi-equilibrium states for spherical and cylindrical micelles. The slowest stage is the stage with a joined quasi-equilibrium for spherical and cylindrical micelles. This stage was observed for all considered cases, including micellization. The time scales for similar substages of fast and slow relaxation at large initial excess and deficit of surfactant monomers are the same.

We have shown that the results of the difference Becker-Döring kinetic equations for fast and slow nonlinear relaxation at large initial excess and deficit of surfactant monomers are in fine agreement with predictions of analytical kinetic theory of relaxation for concentration of monomers and total concentrations of spherical and cylindrical micelles.

Let us note that micelle formation/breakdown processes can be reversed by corresponding change of the monomer concentration. We have considered here micellization where any aggregates with aggregation number $n > 1$ initially were absent. Our study in section 2 and 3 showed that at sufficiently high initial monomer concentration in the vicinity and above the cmc_2, spherical micelles are formed consequently from monomers, and then part of spherical micelles transforms into cylindrical micelles. The reverse process was observed in the case of large initial deficit of surfactant monomers in comparison to the final equilibrium state of the micellar system considered in section 4. The number of cylindrical micelles diminishes in this case while the number of spherical micelles grow. Thus our approach works for both the sphere-to-cylinder and the cylinder-to-sphere transitions, demonstrating their barrier dependence on the surfactant monomer concentration. This is in agreement with known coarse-grained molecular dynamics simulations for pentaethylene glycol monodecyl ether in aqueous solution[42]. As we noted previously, we did not consider here other fission mechanisms of breaking the long cylindrical micelles which can be of importance in the case of micelles made of amphiphilic block copolymers.[43] It could be a subject of future work.

Unfortunately, it is impossible at this moment to compare our results with that from experiments on dynamics of coexisting spherical and cylindrical micelles. There is experimental evidence concerning co-existence of spherical and rod-like micelles obtained with the help of cryo-TEM technique,[44] dynamic light scattering,[45,46] and time-resolved small angle X-ray and neutron scattering techniques.[47,48] These data is related to equilibrium states of nonionic and ionic direct micelles and non-equilibrium cylinder-to-sphere transitions in block copolymer micelles. Although specific relaxation times and rate constants for spherical and separately for cylindrical micelles breakdown had been measured,[4,18] however there were no experiments on total time evolution of the systems with coexisting spherical and cylindrical direct nonionic micelles.

Nevertheless, such experiment can be designed. The most appropriate for that could be synchrotron small-angle X-ray scattering in combination with the stopped-flow mixing technique. Recently this approach has successfully been applied for study of micelle formation at rapid mixing of a solution of dissolved dodecyl maltoside in dimethylformamide with water.[49] Such experiment allows one to control the changing concentrations of aggregates with different aggregation numbers and shapes under arbitrary initial conditions. It is just our case.

Acknowledgements

This work was supported by St. Petersburg State University (grant 11.37.183.2014) and grant of Russian Foundation for Basic Research 13-03-00991a. N. Volkov thanks St.Petersburg State University for his employment within the University Postdoctoral Program (grant 11.50.1609.2013).

Notes and references

[a] Department of Statistical Physics, Faculty of Physics, St Petersburg State University, Ulyanovskaya 1, Petrodvoretz, St Petersburg, 198504, Russian Federation.

1 M.J. Rosen and J.T. Kunjappu, *Surfactants and Interfacial Phenomena*, 4th ed. (John Wiley & Sons, Inc.: Hoboken, NJ, 2012).
2 K. Holmberg, B. Jonsson, B. Kronberg and B. Lindman, *Surfactants and Polymers in Aqueous Solution*, 2nd ed. (John Wiley & Sons, Ltd: New York, 2002).
3 A.I. Rusanov, *Micellisation in Surfactant Solutions* (*Chemistry Reviews*), Taylor & Francis, 1998.
4 R. Zana, Dynamics in Micellar Solutions of Surfactants. In *Dynamics of Surfactant Self-Assembles, Micelles, Microemulsions, Vesicles, and Lyotrophic Phases,* Surfactant Science Series Vol.125, edited by R. Zana (Taylor & Francis, Boca Raton, 2005), Ch. 3, p.75.
5 A.K. Shchekin, F.M. Kuni, A.P. Grinin, A.I. Rusanov, Nucleation in micellisation processes. In *Nucleation Theory and Applications*, edited by J.W.P. Schmelzer (Wiley: New York, 2005), Ch.9, p. 312.
6 R. Becker and W. Döring, *Ann. Phys.*,1935, **24**, 719.
7 J.C. Shelley and M.Y. Shelley, *Current Opinion in Colloid & Interface Science*, 2000, **5**, 101.
8 E. N. Brodskaya, *Colloid Journal*, 2012, **74**, 154.

[9] D. T. Gillespie, *J. Phys. Chem*., 1977, **81**, 2340.
[10] F. Mavelli and M. Maestro, *J. Chem. Phys.*, 1999, **111**, 4310.
[11] S.-J. Marrink, D. P. Tieleman, A. E. Mark, *J. Phys. Chem.* B, 2000, **104**, 12165.
[12] E. A. G. Aniansson and S. N. Wall, *J. Phys. Chem.*, 1974, **78**, 1024.
[13] E. A. G. Aniansson and S. N. Wall, *J. Phys. Chem.*, 1975, **79**, 857.
[14] G. Mohan and D. I. Kopelevich, *J. Chem.Phys.,* 2008, **128**, 044905.
[15] V. Starov, V. Zhdanov, N.M. Kovalchuk, *Colloids and Surfaces A: Physicochem. Eng. Aspects*, 2010, **354**, 268.
[16] M. Almgren, E. A. G. Aniansson and K. Holmaker, *Chem. Phys.*, 1977, **19**, 1.
[17] M. Teubner, *J. Phys. Chem.*, 1979, **83**, 2917.
[18] M. Kahlweit and M. Teubner, *Adv. Colloid Interface Sci.*, 1980, **13**, 1.
[19] S. N. Wall and E. A. G. Aniansson, *J. Phys. Chem.*, 1980, **84**, 727.
[20] A. P. Grinin and D. S. Grebenkov, *Colloid Journal*, 2003, **65**, 552.
[21] F.M. Kuni, A.I. Rusanov, A.K. Shchekin and A.P. Grinin, *Russ. J. Phys. Chem.*, 2005, **79**, 833.
[22] A.K. Shchekin, F.M. Kuni and K.S. Shakhnov, *Colloid J.*, 2008, **70**, 244.
[23] I.M. Griffiths, C.D. Bain, C.J.W. Breward, D.M. Colegate, P.D. Howell and S.L. Waters*, J. Colloid and Interface Sci.*, 2011, **360**, 662.
[24] I.M. Griffiths, C.D. Bain, C.J.W. Breward, S.J. Chapman, P.D. Howell and S.L. Waters, *SIAM Journal on Applied* Mathematic, 2012, **72**, 201.
[25] I.A. Babintsev, L.Ts. Adzhemyan and A.K. Shchekin, *J. Chem. Phys*., 2012, **137**, 044902.
[26] S. Wall and C. Elvingson, *J. Phys. Chem*., 1985, **89**, 2695.
[27] C. Elvingson and S. Wall, *J. Phys. Chem*., 1986, **90**, 5250.
[28] F.M. Kuni, A.K. Shchekin, A.I. Rusanov and A.P. Grinin, Langmuir, 2006, **22**, 1534.
[29] M.S. Kshevetskii, A.K. Shchekin and F.M. Kuni, Colloid J. **70**, 455 (2008).
[30] A.K. Shchekin, F.M. Kuni, A.P. Grinin, A.I. Rusanov, *Russ. J. Phys. Chem.* A, 2008, **82**, 101.
[31] M.S. Kshevetskiy and A.K. Shchekin, *J. Chem. Phys.*, 2009, **131**, 074114.
[32] A.K. Shchekin, A.I. Rusanov and F.M. Kuni, *Chemistry Letters*, 2012, **41**, 1081.
[33] I.M. Griffiths, C.J.W. Breward, D.M. Colegate, P.J. Dellar, P.D. Howell and C.D. Bain, *Soft Matter* 2013, **9**, 853.
[34] I.A. Babintsev, L.Ts. Adzhemyan and A.K. Shchekin, *Soft Matter*, 2014, **10**, 2619 (2014).
[35] I.A. Babintsev, L.Ts. Adzhemyan and A.K. Shchekin, *J. Chem. Phys*., 2014, **141**, 064901.
[36] G. Porte, Y. Poggi, J. Appell and G. Maret, *J. Phys. Chem*., 1984, **88**, 5713.
[37] S. May and A. Ben-Shaul, *J. Phys. Chem. B*, 2001, **105**, 630.
[38] S. May and A. Ben-Shaul, Molecular Packing in Cylindrical Micelles. In: *Giant Micelles: Properties and Applications* R. Zana and E. Kaler, Eds. (CRC Press: Boca Raton, 2007), p.41.
[39] A. I. Rusanov, F. M. Kuni, A. P. Grinin, and A. K. Shchekin, *Colloid J.*, 2002, **64**, 605; A. I. Rusanov, A. P. Grinin, F. M. Kuni, and A. K. Shchekin, *Russ. J. Gen. Chem.*, 2002, **72**, 607.
[40] A.G. Daful, V.A. Baulin, J.B. Avalos, and A.D. Mackie, *J. Phys. Chem. B*, 2011, **115**, 3434.
[41] M. Smoluchowski, *Phys. Chem.*, 1917, **92**, 129.
[42] M. Velinova, D. Sengupta, A.V. Tadjer, and S.-J. Marrink, *Langmuir*, 2011, **27**, 14071.
[43] Q. Chen, Y. Li, C. Wu, Macromolecules, 2013, **46**, 9164.
[44] A.Khan, A. Kaplun, Y. Talmon, and M. Hellsten, *J. Colloid Interface Sci*., 1996, **181**, 191.
[45] P.R. Majhi, P.L. Dubin, X. Feng, and X. Guo, *J. Phys. Chem. B*, 2004, **108**, 5980.
[46] T.G. Movchan, I.V. Soboleva, E.V. Plotnikova, A.K. Shchekin, and A.I. Rusanov, *Colloid J.*, 2012, **74**, 239.
[47] R. Lund, L. Willner, D. Richter, P. Lindner, and T. Narayanan, *ACS Macro Lett.*, 2013, **2**, 1082.
[48] R. Lund, L. Willner, and D. Richter, *Adv. Polymer Sci.*, 2013, **259**, 51.
[49] G.V. Jensen, R. Lund, J. Gummel, M. Monkenbusch, T. Narayanan, and J.S. Pedersen, *J. Am. Chem. Soc.*, 2013, **135**, 7214.|

Manuscript ID RA-ART-08-2014-008683
Title: Kinetic modeling of aggregation in solutions with coexisting spherical and cylindrical micelles at arbitrary initial conditions

Table of contents:

* Colour graphic: maximum size 8 cm x 4 cm

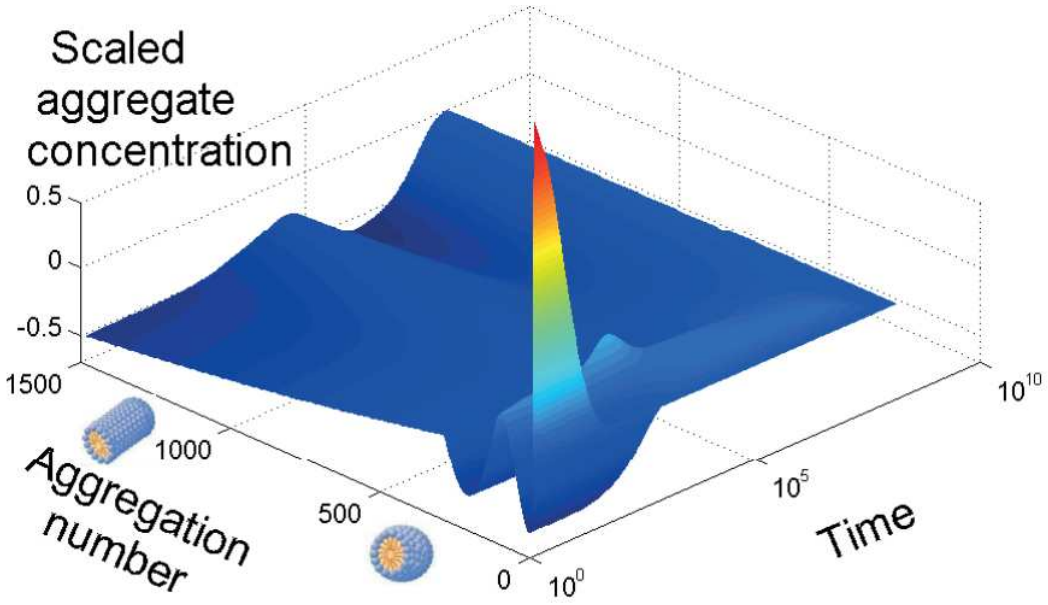

* Text: one sentence, of maximum 20 words, highlighting the novelty of the work.

The whole picture of evolution of coexisting spherical and cylindrical micelles has been described for initial states far from equilibrium.